
Strategic Classification with Non-Linear Classifiers

Benyamin Trachtenberg, Nir Rosenfeld
 Technion – Israel Institute of Technology
 Haifa, Israel
 {benyamint, nirr} @cs.technion.ac.il

Abstract

In strategic classification, the standard supervised learning setting is extended to support the notion of strategic user behavior in the form of costly feature manipulations made in response to a classifier. While standard learning supports a broad range of model classes, the study of strategic classification has, so far, been dedicated mostly to linear classifiers. This work aims to expand the horizon by exploring how strategic behavior manifests under non-linear classifiers and what this implies for learning. We take a bottom-up approach showing how non-linearity affects decision boundary points, classifier expressivity, and model classes complexity. A key finding is that universal approximators (e.g., neural nets) are no longer universal once the environment is strategic. We demonstrate empirically how this can create performance gaps even on an unrestricted model class.

1 Introduction

Strategic classification considers learning in a setting where users modify their features in response to a deployed classifier to obtain positive predictions [3, 4, 16]. This setting aims to capture a natural tension that can arise between a system aiming to maximize accuracy, and its users who seek favorable outcomes. Such a tension is well-motivated across diverse applications including loans approval, university admissions, job hiring, welfare and education programs, and medical services. The field has drawn much attention since its introduction, leading to advances along multiple learning fronts such as generalization [6, 31, 34], optimization [24], loss functions [23, 25], and extensions [11, 14, 18, 28].

However, despite over a decade of efforts, research in strategic classification remains focused predominantly on learning with linear classifiers. Given the inherent challenges of learning in a strategic environment, linearity has the benefit of inducing a simple form of strategic behavior that permits tractable analysis. Because many realistic applications—including those mentioned above—make regular use of non-linear models, we believe that it is important to establish a better understanding of how non-linearity shapes strategic behavior, and how behavior in turn affects learning. Our paper therefore aims to extend the study of strategic classification to the non-linear regime in the hopes of developing the necessary understanding for future learning in this setting.

Our first observation is that non-linear classifiers induce qualitatively different behavior than linear ones in the strategic setting. Consider first the structure induced by standard linear classifiers. Generally, users in strategic classification are assumed to best-respond to the classifier by modifying their features in a way that maximizes utility (from prediction) minus costs (from modification). For a linear classifier h coupled with the common choice of an ℓ_2 cost, modifications $x \mapsto x^h$ manifest as a projection of x onto the linear decision boundary of h if this incurs less than a unit cost. This simple form has several implications. First, note that all points ‘move’ in the same direction, making strategic behavior, in effect, uni-dimensional. Second, the region of points that move forms a band of unit distance on the negative side of h . This means that the set of points classified as positive forms a halfspace, which implies that the ‘effective’ classifier, given by $h_\Delta(x) := h(x^h)$, is also linear. Third, and as a result, the induced effective model class remains linear.

Together, the above suggest that for linear classifiers coupled with ℓ_2 costs, the transition from the standard, non-strategic setting to a strategic one requires anticipating which points move, but otherwise remains similar. One known implication is that the strategic and non-strategic VC dimension of linear classifiers are the same [31]. Furthermore, the Bayes-optimal strategic classifier can be derived by taking the optimal non-strategic classifier and simply increasing its bias term by one [27]. Note this means that any linearly separable problem remains separable, and that strategic classifiers can, in principle, attain the same level of accuracy as their non-strategic counterparts. Thus, while perhaps challenging to solve in practice, the intrinsic difficulty of strategic linear classification remains unchanged.

The above, however, is unlikely to hold for non-linear classifiers: once the decision boundary is non-linear, different points will move in different directions. In addition to the possible distortion of the shapes of each individual classifier, the effective (i.e., strategic) model class may also change, which can have concrete implications on expressivity, generalization, optimization, and attainable accuracy. This motivates the need to explore how strategic responses shape outcomes in non-linear strategic classification, which we believe is crucial as a first step towards developing future methods. Our general approach is to examine—through analysis, examples, and experiments—how objects in the original non-strategic task map to corresponding objects in the induced strategic problem instance. Initially, our conjecture was that strategic behavior acts as a ‘smoothing’ operator on the original decision boundary, but as we show, the actual effect of strategic behavior turns out to be more involved.

Taking a bottom-up approach, we study three mappings between (i) individual points, (ii) classifiers, and (iii) model classes. For points, we begin by showing that the mapping is not necessarily bijective. As a result, some points on the original decision boundary become ‘wiped out’, while others are ‘expanded’ to become intervals (arcs for ℓ_2 costs) on the induced boundary. We demonstrate several mechanisms that can give rise to both phenomena. For classifiers, we show how the effects on individual points aggregate to modify the entire decision boundary. A key finding is that certain decision boundaries are *impossible to express* under strategic behavior. We give several examples of reasonable classifier types that cannot exist under strategic behavior, and show that some effective classifiers h_Δ can be traced back to (infinitely) many original classifiers h . The main takeaway is that universal approximators, such as neural networks or RBF kernels, are no longer universal in a strategic environment.

For model classes, our results build on the observation that the mapping from original to effective classifiers *within* the class is non-bijective. In particular, because many h can be mapped to the same h_Δ , the VC dimension of the induced model class can shrink even from ∞ down to 0, causing model classes that were not learnable in the standard setting to become learnable in the strategic one. That said, the VC dimension of the induced class can generally either grow, or shrink. We highlight some conditions that guarantee either of these outcomes, though we conjecture that there is a bound on how much complexity can grow. We conclude with experiments that shed light on how strategic behavior may alter the effective complexity and maximum accuracy of the learned model class in practice.

2 Related work

Our work focuses on the common setting of supervised binary classification, where non-linear models are highly prevalent in general. This follows the original formulation of strategic classification [3, 16], which has since been extended also to online settings [1, 5, 8] and to regression [2, 29]. As noted, linear models have thus far been at the forefront of the field, with many works relying (explicitly or implicitly) on their properties or induced structure [5, 10, 18, 24, 27]. Even for works with results agnostic to model class, linear classifiers remains the focus of special-case analyses, examples, and empirical evaluation [19, 25, 35], and their generality does not shed light on the impact of non-linearity. Other works offer only tangential results, such as welfare analysis in the non-linear setting [33], but do not paint a picture of the general learning problem. Technically related, the field of offset curves deals with distortions of general non-linear curves, though it is ultimately more concerned with approximation and analytical properties and does not convey direct implications for learning [12, 20]. In terms of theory, both [31, 34] apply PAC analysis to strategic classification, the latter providing VC bounds for the linear class. Most relevant to us is [6] who study the general learnability of strategic learning under different feedback models. While not restricted to particular classes, their analysis depends crucially on the assumption that each user can move only to a finite set of possible points whose cardinality plays an explicit role. Our work tackles the more pervasive setting of movement governed by cost functions, and is therefore continuous. The above works focus primarily on statistical hardness; while this is also one of our aims, we are interested in establishing a broader understanding of the non-linear regime.

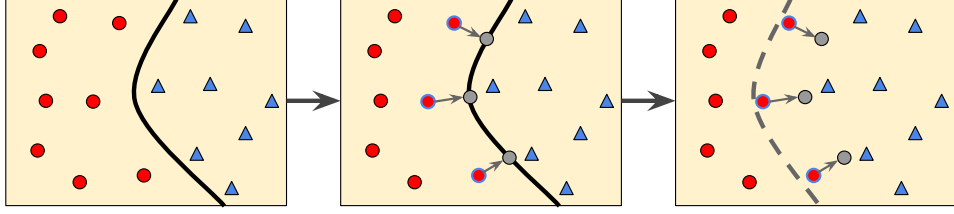


Figure 1: **(Left)** Original non-linear classifier h . **(Middle)** Strategic response to original classifier. **(Right)** Resulting effective classifier h_Δ (different from h) after accounting for strategic responses.

3 Preliminaries

We work in the original supervised setting of strategic classification [3, 16]. Let $x \in \mathcal{X} = \mathbb{R}^d$ denote user features, $y \in \mathcal{Y} = \{0, 1\}$ their corresponding label, and assume pairs (x, y) are drawn iid from some unknown joint distribution D . Given a training set $T = \{(x_i, y_i)\}_{i=1}^m \sim D^m$, learning aims for the common goal of finding a classifier $h \in H$ that maximizes expected predictive accuracy, where H is some chosen model class. The unique aspect of strategic classification is that at test time, users modify their features to maximize gains in response to the learned h via the *best-response mapping*:

$$x^h := \Delta_h(x) = \operatorname{argmax}_{x'} \alpha h(x) - c(x, x') \quad (1)$$

where α determines their utility from obtaining a positive prediction $\hat{y} = h(x)$, and c is a function governing modification costs. We assume w.l.o.g. that the user gains no utility from a negative prediction. Like most works, we focus mainly on the ℓ_2 cost, i.e., $c(x, x') = \|x - x'\|_2$, but discuss other costs in a subset of our results. Because no rational user will pay more than α , x^h will always be contained in the ball of radius α around x denoted $B_\alpha(x) = \{x' : c(x, x') \leq \alpha\}$. It will also be useful to define the corresponding sphere, $S_\alpha(x) = \{x' : c(x, x') = \alpha\}$.

Given the above, the learning objective is to maximize expected *strategic accuracy*, defined as:

$$\operatorname{argmax}_{h \in H} \mathbb{E}_D[\mathbb{1}\{y = h(\Delta_h(x))\}] \quad (2)$$

Levels of analysis. We assume w.l.o.g. that classifiers are of the form $h(x) = \mathbb{1}\{f(x) \geq 0\}$ for some scalar score function f and that the decision boundary is then the set of points for which $f(x) = 0$. Our analysis takes a ‘bottom-up’ approach in which we first consider changes to individual points on the boundary; then ask how such local changes aggregate to affect a given classifier h ; and finally, how these changes impact the entire model class H . It will therefore be useful to consider three mappings between original and corresponding strategic objects. For points, the mapping is $x \mapsto \nabla_h(x) = \{x' : \Delta_h(x') = x \wedge c(x, x') = \alpha\}$, i.e. the set of points x' that, in response to h , move to x at maximal cost. For classifiers, we define the *effective classifier* as $h_\Delta(x) := h(\Delta_h(x))$ (see Fig. 1), and consider the mapping $h \mapsto h_\Delta$. This allows us to compare the original decision boundary of h to the ‘strategic decision boundary’ of its induced h_Δ , since both are defined w.r.t. raw (unmodified) inputs x . For model classes, we consider $H \mapsto H_\Delta := \{h_\Delta : h \in H\}$, and refer to H_Δ as the *effective model class*.

The linear case. As noted, most works in strategic classification consider H to be the class of linear classifiers, $h(x) = \mathbb{1}\{w^\top x \geq b\}$. A known result is that $\Delta_h(x)$ can be expressed in closed form as a conditional projection operator: x moves to $x_{\text{proj}} = x - \frac{w^\top x - b}{\|w\|_2^2} w$ if $h(x) = 0$ and $c(x, x_{\text{proj}}) \leq \alpha$, and otherwise remains at x [9]. Note that all points that move do so in the same direction, i.e., orthogonally to w . Furthermore, each x on the decision boundary of h is mapped to the single point \hat{x} at an orthogonal distance (or cost) of exactly α . Considering this for all boundary points, we get that h_Δ simply shifts the decision boundary by α , which gives $h_\Delta(x) = \mathbb{1}\{w^\top x \geq b - \alpha\}$. As a result, H_Δ remains the set of all linear classifiers, and so $H_\Delta = H$.

The non-linear case: first steps. Informally stated, the main difference for non-linear classifiers is that points no longer move in the same direction (see Fig. 1). Note that while points still move to the ‘closest’ point on the decision boundary, the projection operator is no longer nicely defined. The result is that the shape of the decision boundary of h may not be preserved when transitioning to h_Δ . Moreover, and as we will show, some points on the decision boundary of h will “disappear” and have

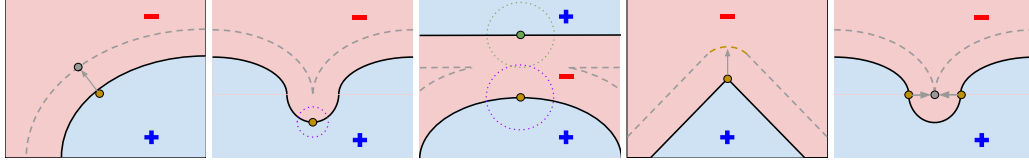


Figure 2: **Types of point mappings.** From left to right: one-to-one, direct wipeout, indirect wipeout, expansion, and collision. Black lines show original h , dashed grey lines indicate h_Δ , and dotted circles show $S_\alpha(x)$.

no effect on the induced h_Δ , while other points may be expanded to affect a continuum of points on h_Δ . A final observation is that directionality is important in the strategic setting: because points always move towards the positive region, the shape of h_Δ for some h may be very different than that of the same classifier but with "inverted" predictions, $h'(x) = 1 - h(x)$. This lack of symmetry means that we cannot take for granted that the induced H_Δ will include both h_Δ and $1 - h_\Delta$, even if H does.

4 Points

To gain understanding about what determines the shape of h_Δ of a general h , we begin by considering a single point x on the decision boundary of h and examining how (and if) it maps to corresponding point(s) on the decision boundary of h_Δ through the point mapping $x \mapsto \nabla_h(x)$. We identify and discuss four general cases (see Fig. 2):

Case #1: One-to-one. For linear h , the point mapping is always one-to-one. For non-linear h , the mapping remains one-to-one as long as h is ‘well-behaved’ on x . We consider this the ‘typical’ case and note that each x is mapped to the single point $\hat{x} = x - \alpha \hat{n}_x$, where \hat{n}_x is the unit normal at x w.r.t. h (see Appendix B.1). A necessary condition for one-to-one mapping is that h is smooth at x , but smoothness is not sufficient—as the following cases depict.

Case #2: Wipeout. Even if h is smooth at x , in some cases the point mapping will be null, $x \mapsto \emptyset$. We refer to this phenomenon as *wipeout*, and identify two types. *Direct wipeout* occurs when the signed curvature κ at x is negative and of sufficiently large magnitude; this is defined formally in Sec. 5.1. Intuitively, this results from strategic behavior obfuscating any rapid changes in the decision boundary of h . *Indirect wipeout* occurs when the the set of points $\nabla_h(x)$ is contained in $B_\alpha(x')$ for some other x' on the decision boundary. For both types, the result is that $B_\alpha(x)$ is entirely contained in the positive region of h and such x have no effect on h_Δ (see Appendix B.2).

Case #3: Expansion. When the decision boundary of h at x is not smooth (i.e., a kink or corner), x can be mapped to a continuum of points on the effective boundary of h_Δ . This, however, occurs only when the decision boundary is locally convex towards the positive region. The set of mapped points $\nabla_h(x)$ are those on $S_\alpha(x)$ who do not intersect with any other $B_\alpha(x')$ for other x' on the boundary of h . Thus, the shape of the induced ‘artifact’ is partial to a ball. Partial expansion may occur if some of the expansion artifact is discarded through indirect wipeout (Appendix C.1).

Case #4: Collision. A final case is when a set of points $\{x\}$ on the boundary of h are all mapped to the same single point \hat{x} on h_Δ , i.e., $\nabla_h(x) = \nabla_h(x') = \hat{x}$ for all x, x' in the set. Typically, this happens at the transitions between well-behaved decision boundary segments and wiped-out regions. Collision often results in non-smooth kinks on h_Δ , even if all source points were smooth on h .

5 Classifiers

We now turn to examine how strategic behavior affects the classifier mapping $h \mapsto h_\Delta$. We identify two mechanisms that can limit expressivity of effective classifiers: curvature, and containment.

5.1 Curvature

To understand the mapping $h \mapsto h_\Delta$, it will be useful to first examine what happens to boundary points x in terms of how h behaves around them. We make use of the notion of *signed curvature*, denoted κ , which quantifies how much the decision boundary deviates from being linear at a certain

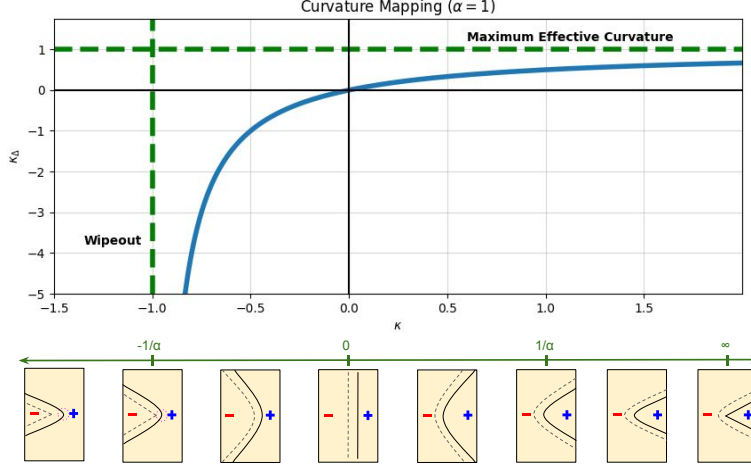


Figure 3: **(Top)** Graph of Eq. 3 with asymptotes represented as dashed lines. **(Bottom)** Depictions of curvature mappings for increasing κ .

point x . For $d = 2$, curvature is formally defined as $\kappa = 1/r$ where r is the radius of the circle that best approximates the curve at x . For $d > 2$, we use $\kappa^* = \sup(K)$ where K includes all directional curvatures at x (see Appendix A.1). The sign of κ measures whether the decision boundary bends (i.e., is convex) towards the positive region ($\kappa > 0$), the negative region ($\kappa < 0$), or is locally linear ($\kappa = 0$).

Let x be a typical point on the decision boundary of h which satisfies the one-to-one mapping detailed in Sec. 4. Our next result (which relies on an equivalent form in the field of offset curves [12]) characterizes the *effective signed curvature* of h_Δ at \hat{x} , denoted κ_Δ , as a function of the curvature κ of h at x .

Proposition 1. *Let x be a point on the decision boundary of h with signed curvature $\kappa \geq -1/\alpha$. The effective curvature of the corresponding \hat{x} on the boundary of h_Δ is given by:*

$$\kappa_\Delta = \kappa / (1 + \alpha\kappa) \quad (3)$$

When $d > 2$, each curvature in K is mapped as in Eq. 3 to form $K_\Delta = \{\kappa / (1 + \alpha\kappa) : \kappa \in K\}$, and κ_Δ^* follows. See Appendix B.3 for proof and Fig. 3 for an illustration of how this impacts the shape of h_Δ . Prop. 1 entails several interesting properties. First, strategic behavior preserves the direction of curvature, i.e., $\kappa \cdot \kappa_\Delta \geq 0$ always. In particular, $\kappa = 0$ entails $\kappa_\Delta = 0$, which explains why linear functions remain linear. Second, effective curvature κ_Δ is monotonically increasing in κ , concave, and sub-linear. This implies that for $\kappa > 0$ the effective positive curvature *decreases*, while for $\kappa < 0$ the effective negative curvature *increases*. Thus, strategic behavior acts as a *directional smoothing operator*, i.e., the boundaries' rate of change is expected to decrease but only in the positive direction.

Finally, in the positive direction, κ_Δ is bounded from above, approaching $1/\alpha$ as $\kappa \rightarrow \infty$. This gives:

Observation 1. *No effective classifier h_Δ can have positive curvature κ_Δ greater than $1/\alpha$.*

When $d > 2$, Obs. 1 holds for each curvature $\kappa \in K$ and can be summarized as $\kappa_\Delta^* \leq 1/\alpha$. Though Prop. 1 only implies Obs. 1 at points on h_Δ that are typical, we will show in Sec. 5.3 that is also true at any point on h_Δ . The above holds irrespective of the shape and curvature of the original h . In particular, non-smooth points on h (i.e., with $\kappa \rightarrow \infty$), such as an edge or vertex at the intersection of halfspaces, becomes smooth on h_Δ . Conversely, in the negative direction, κ_Δ approaches $-\infty$ as $\kappa \rightarrow -1/\alpha$. Thus, negative curvature can grow arbitrarily large, and at $\kappa = -1/\alpha$ maps to a non-smooth "kink" in h_Δ . κ_Δ is no longer defined when κ crosses the asymptote at $-1/\alpha$ because such points are wiped out and have no corresponding \hat{x} on the boundary of h_Δ . This is the exact case of *indirect wipeout* in Sec. 4 (see Appendix B.2 for proof).

Observation 2. *Any point x on the decision boundary of h with curvature $\kappa < -1/\alpha$ has no influence on h_Δ . In higher dimensions, this is true for any point x with $\inf(K) < -1/\alpha$.*

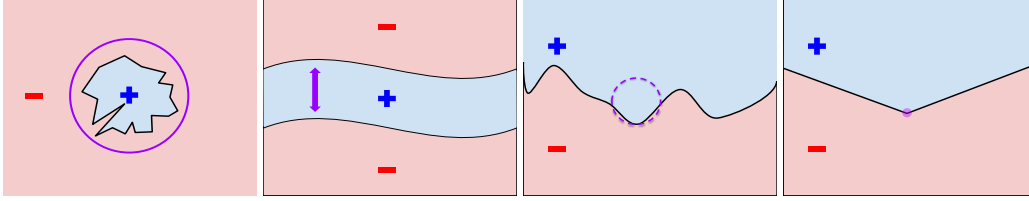


Figure 4: **Types of impossible effective classifiers.** From left to right: small positive region, narrow positive strip, large positive curvature, piecewise (hyper)linear convex towards positive region.

5.2 Containment

Because the decision boundary is a level set of some score function f , contained regions are not only possible, but realistic. Consider a given classifier h where the decision boundary forms some bounded connected negative region $C \subset \mathbb{R}^d$ where $h(x) = 0 \forall x \in C$. Strategic behavior dictates that negative areas shrink, and as such, only a subset of C will still be classified as negative in h_Δ . If C is sufficiently small, then it will disappear completely leaving $h_\Delta(x) = 1 \forall x \in C$.

Observation 3. Any negative region C fully contained in some $B_\alpha(x)$ will become positive in h_Δ .

The fact that positive areas grow and negative areas shrink also implies that there is a minimum size positive region that can exist in any h_Δ . This idea will be formalized and generalized later in Sec. 5.3. Another observation is that when negative regions are wiped out, two or more positive regions may merge leading to a less expressive decision boundary. On the other hand, the strategic setting can also split a negative region creating a more expressive decision boundary. For example, if h induces a negative connected region C whose shape is formed by two large regions connected by a narrow "strait", the strait will be wiped out leaving two disjoint components (see Appendix C.2).

Observation 4. Strategic behavior can merge positive regions and split negative regions thereby either increasing or decreasing the number of connected regions (either positive or negative).

5.3 Impossible effective boundaries

Based on the above, we derive two general statements about effective classifiers that cannot exist. Each statement considers some candidate classifier g , and shows that if g satisfies a certain property, then there is no classifier h for which g is its induced effective classifier, i.e., $g \neq h_\Delta$ for any h .

We require some additional notation. Given h , define the set of negatively classified points as $\mathcal{X}_0(h) = \{x : h(x) = 0\}$. For a set $A \subseteq \mathcal{X}$, we say a point x is *reachable* from A if $\exists x' \in A : c(x, x') \leq \alpha$.

Proposition 2. Let g be a candidate classifier. If there exists a point x on the decision boundary of g such that all points $x' \in S_\alpha(x)$ are reachable from some point in $\mathcal{X}_0(g)$, then there is no h such that $g = h_\Delta$.

The intuition behind Prop. 2 is that g cannot simultaneously classify x as positive while also classifying all $y \in \mathcal{X}_0$ as negative. Full proof in Appendix B.4. As stated in Prop. 3, when g is smooth at x , Prop. 2 can be simplified to require that only a single point be checked instead of all of $S_\alpha(x)$.

Proposition 3. Let g be a candidate classifier. If there exists a point x on the decision boundary of g where (i) g is smooth, and (ii) the point $\hat{x} = x + \alpha \hat{n}_x$ is reachable by some other $x' \in \mathcal{X}_0(g)$, then there is no h such that $g = h_\Delta$.

The intuition behind Prop. 3 is the same as for Prop. 2 except that when g is smooth at x , the only point in $S_\alpha(x)$ that may not be reachable by some $x' \in \mathcal{X}_0(g)$ is $\hat{x} = x + \alpha \hat{n}_x$ (see Appendix B.5).

Examples. The implication of Props. 2 and 3 is that there exist decision boundaries which are generally realizable, but are no longer realizable as effective classifiers in the strategic setting. Note that because it only takes a single decision boundary point to render an entire effective classifier infeasible, each of these examples are broad categories and pose meaningful restrictions on the set of possible effective classifiers. We highlight four types of impossible effective decision boundaries:

1. Classifiers with a small positive region that can be enclosed by a ball of radius α .



Figure 5: **(Left)** Example of increasing VC. **(Right)** Example of a dataset with limited strategic accuracy. Any h_Δ which correctly classifies the gold-rimmed point must err on a negative point.

2. Classifiers with a narrow positive region in which points are α -close to the decision boundary.
3. Classifiers with large positive signed curvature anywhere on the decision boundary.
4. Classifiers with any locally convex piecewise linear or hyperlinear segments.

These are illustrated in Fig. 4. Proofs in Appendix C.3, and either build on Obs. 1-4, or show the conditions of Props. 2 or 3 hold. From these four example, we note the following observation.

Observation 5. *The mapping $h \mapsto h_\Delta$ is not bijective, with many candidate h_Δ having no corresponding h and many h mapped to the same h_Δ .*

In Appendix C.4 we show that there are actually infinite h that map to nearly all possible h_Δ . Furthermore, Obs. 5 will be important to proving Thm. 1 and Cor. 1

6 Model classes

On the classifier level, the strategic setting is clearly more restrictive than the regular setting. Indeed, in Sec. 6.2 we will extend this idea into the model class level by analyzing the impacts on universality and optimal accuracy. However, as we show in 6.1 the model class mapping is more nuanced than the classifier mapping since complexity can actually increase as a result of strategic behavior.

6.1 Class complexity

Recall that for linear classes, H_Δ remains linear and so $H \mapsto H_\Delta = H$. Although this equivalence is not unique to the class of linear classifiers (see examples in Appendix C.5), typically, we can expect strategic behavior to alter the complexity of the induced class. Here, we use VC analysis to shed light on this effect by examining the possible relations between $VC(H)$ and $VC(H_\Delta)$.¹

Complexity reduction. Since our results so far point out that effective classifiers are inherently constrained, a plausible guess is that effective complexity should decrease. Indeed, there are some natural classes where VC cannot increase. For example:

Proposition 4. *For each class Q_s^k of negative-inside k -vertex polytopes bounded by a radius of s , $VC(Q_s^k) \geq VC(Q_{s,\Delta}^k)$. Moreover, if $s = \infty$, then $VC(Q_s^k) = VC(Q_{s,\Delta}^k)$ as implied by Thm. 2.*

Proof in Appendix B.7. Curiously, in some extreme cases, the reduction spans the maximum extent.

Theorem 1. *There exist several model classes H where $VC(H) = \infty$, but $VC(H_\Delta) = 0$.*

Proof in Appendix B.8. See Appendix C.6 for other examples where VC strictly decreases yet does not diminish completely. Thm. 1 carries concrete implications for strategic learning:

Corollary 1. *A model class that is not learnable in the regular setting may become learnable in strategic environments.*

Complexity increase. While lower effective VC is indeed a possibility, the effective complexity generally stays the same or increases. As an intuition for how the VC might increase, consider the simple example in Fig. 5 (left). Here H includes 4 non-overlapping classifiers with $VC(H) = 1$, yet under strategic behavior, the effective classifiers overlap increasing the shattering capacity to 2. This case can be generalized to give $VC(H_\Delta) = \theta(d \cdot VC(H))$ (see Appendix C.7). We next

¹This aligns with the notion of *strategic VC* used in [21, 31], i.e., $SVC(H) \equiv VC(H_\Delta)$.

identify a simple generic sufficient condition for the effective complexity of any learnable class to be non-decreasing. The proof of Thm. 2 can be found in Appendix B.9.

Theorem 2. *If H is closed under input scaling and $\text{VC}(H) < \infty$, then $\text{VC}(H) \leq \text{VC}(H_\Delta)$.*

This applies to many common classes, such as polynomials, polytopes, and most neural networks. In the case of polytopes (positive-inside), we can also upper bound the VC of the effective class.

Theorem 3. *Consider either the ℓ_1 , ℓ_2 , or ℓ_∞ costs and let $H \subseteq P^k$, where P^k is the set of all k -vertex polytopes in \mathbb{R}^d . Then $\text{VC}(H_\Delta) = O(kd^2 \log k)$.*

Proof is in Appendix B.10. Since it is known that $\text{VC}(P^k) = O(kd^2 \log k)$ [22], Thm. 3 suggests that the effective VC dimension can increase, but potentially only to a limited extent as in this case where it remains in the same order. For ℓ_1 and ℓ_∞ , note the effective class remains within the polytope family, but with additional vertices (see Appendix B.6). For ℓ_2 , the bound holds despite H_Δ no longer including only polytopes (since corners in h can become "rounded" in h_Δ).

As a follow-up to Thm. 3 and Cor. 1, it is natural to wonder if there is a maximum to how much $\text{VC}(H_\Delta)$ can grow? Despite our best efforts, we could not find any class with bounded VC whose effective VC becomes unbounded, and therefore suspect such classes do not exist.

Conjecture 1. *It is likely that for any norm cost, if H is learnable, then H_Δ is also learnable.*

If proven, this would extend the result of Cohen et al. [6] in the special case of finite manipulation graphs to the more common setting of explicit cost functions (where the graph is continuous).²

6.2 Universality and Approximation

Our results in Sec. 5.3 indicate four "types" of decision boundaries that cannot be attributed to any effective classifier, though others may exist. This implies that several basic classifiers are not realizable in the strategic setting and cannot be approximated well; a simple example is one that classifies some $B_{0.9\alpha}(x)$ as positive and is negative elsewhere. This drives our principle conclusion:

Corollary 2. *Any universal approximator class H is no longer universal under strategic behavior.*

Common examples of universal approximator classes include polynomial thresholds [30], RBF kernel machines [26], many classes of neural networks [e.g., 17], and gradient boosting machines [13]. In the strategic setting, these classes are no longer all-encompassing like in the standard setting.

Approximation gaps. Cor. 2 implies that even if the data is in itself realizable, and even without any limitations on the hypothesis class, the learner may already start off with a bounded maximum training accuracy simply by learning in the strategic setting; see example in Fig. 5 (right) for an example dataset with limited maximum accuracy. This is because strategic behavior makes it impossible to generally approximate intricate functions, e.g., by using fast-changing curvature (via increased depth) or many piecewise-linear segments (with ReLUs). Another result is that the common practice of interpolating the data using highly expressive over-parametrized models (e.g., as in deep learning) is no longer a viable approach. On the upside, it may be possible for the strategic responses to prevent unintentional overfitting, allowing for better generalization.

In extreme cases, the gap between the maximum standard accuracy and the maximum strategic accuracy can be quite large. Our next result demonstrates that there are distributions in which despite a maximum standard accuracy of 1, the maximum strategic accuracy falls to the majority class rate.

Proposition 5. *For all d , there exist (non-degenerate) distributions on \mathbb{R}^d that are realizable in the standard setting, but whose strategic accuracy is the majority class rate, $\max_y p(y)$.*

In one dimension, the distribution can be constructed by placing a negative point δ to the left and right of each positive point. In higher dimensions, negative points can be arranged in a \mathbb{R}^d tetrahedron around each positive point. The full proof is in Appendix B.11. Prop. 6 extends this idea to show that there is a distribution whose maximum strategic accuracy approaches $1/2$ as α increases. The general proof is given in Appendix B.12.

²In particular, they show that $\text{VC}(H_\Delta) = \tilde{O}(\text{VC}(H) \cdot \log k)$ where k is the degree of the manipulation graph. Note the bound is vacuous for $k \rightarrow \infty$, and the proof technique does not apply to continuous graphs.

Proposition 6. *There exists a distribution which is realizable in the standard setting, but whose accuracy under any h_Δ is at most $0.5 + \frac{1}{\lceil 2\alpha+1 \rceil}$.*

In practice, we expect the accuracy gap to depend on the distribution. We explore this gap experimentally in Sec. 7. An interesting observation is that in certain non-realizable settings, the maximum strategic accuracy can *exceed* the maximum standard accuracy. (see Appendix C.8).

7 Experiments

To complement our theoretical results, we present two experiments that empirically demonstrate the effects of strategic behavior on non-linear classifiers.

7.1 Expressivity

Following our results from Sec. 6.1 on the change in hypothesis class expressivity, we experimentally test whether the h_Δ of a given random h belongs to a more or less expressive class than h itself. In particular, we focus on k -degree polynomial classifiers and compare the degree k of h to the degree k_Δ of the polynomial approximation of h_Δ .³ Because user features are often naturally bounded, we assume that $x \in \mathcal{X} = \mathbb{R}^2$ and that x is bounded by $\|x\|_\infty \leq 100$. See Appendix D.1 for full details.

Fig. 6 (left) shows results for varying $k \in [1, 10]$ and for $\alpha \in [2, 40]$. When α is small, we find that $k_\Delta \approx k$, meaning that strategic behavior has little impact on expressivity. However, as α increases, k_Δ becomes larger than k , suggesting that h_Δ is more complex than h . This is due to the fact that as α increases, point mapping collisions (see Sec. 4) become more likely causing non-smooth cusps – which are more complex than basic polynomials – to form in the decision boundary (Fig. 6 (center)). When α is quite large, we see that k_Δ is still larger for low k , but drops considerably for higher k . This can be attributed to the fact that tightly-embedded higher-dimension polynomials and increased strategic reach from large α s are both causes of *indirect wipeout* (see Sec. 4) because they increase the reachability of $\nabla_h(x)$ by other decision boundary points. As such, much of the original decision boundary is wiped out leaving behind a lower complexity effective decision boundary.

7.2 Approximation

As seen in Sec. 6.2, the lack of universality in the strategic setting can impose a limitation on the maximal attainable strategic accuracy. To demonstrate the practical implications of this effect, we upper bound the maximum strategic accuracy of any H_Δ on a set of synthetic data by experimentally calculating the maximum strategic accuracy of the unrestricted effective hypothesis class H_Δ^* . We compare the results to two benchmarks: (i) the standard accuracy of the regular unrestricted hypothesis class H^* (which is always 1), and (ii) the strategic (and standard) accuracy of the linear effective hypothesis class $H_\Delta^{\text{lin}} = H^{\text{lin}}$. The first benchmark measures the amount to which the strategic setting hinders the learner, while the second measures the amount to which the learner can benefit from non-linearity, even in the strategic world. We generate data by sampling points from class-conditional Gaussians $x \sim \mathcal{N}(y\mu, 1)$, and aim to learn an h that obtains an optimal fit. When μ is large, the classes are likely to be well-separated, but when μ is small, points from different classes will be more "interleaved" and thus harder to classify by restricted classes like H_Δ^{lin} and H_Δ^* . Details in Appendix D.1.

Fig. 6 (right) shows results for increasing class separation (μ). As μ decreases and the classification problem becomes more difficult, the maximum strategic accuracy of H_Δ^* diverges from the upper H^* baseline, with performance deteriorating as strategic behavior intensifies (i.e., larger α). Because any actual H_Δ can only have worse performance than the ideal H_Δ^* , this indicates that strategic behavior can become a significant burden in more difficult tasks such as classification in a non linearly-separable setting. Nonetheless, when μ is small, H_Δ^* significantly outperforms the lower H_Δ^{lin} baseline signaling that non-linearities still improve accuracy in the strategic setting despite any strategic effects.

³Though the h_Δ of a k -degree polynomial h is not necessarily a polynomial, we can compare the expressivity of h and h_Δ by finding the lowest k_Δ -degree polynomial g that well-approximates h_Δ .

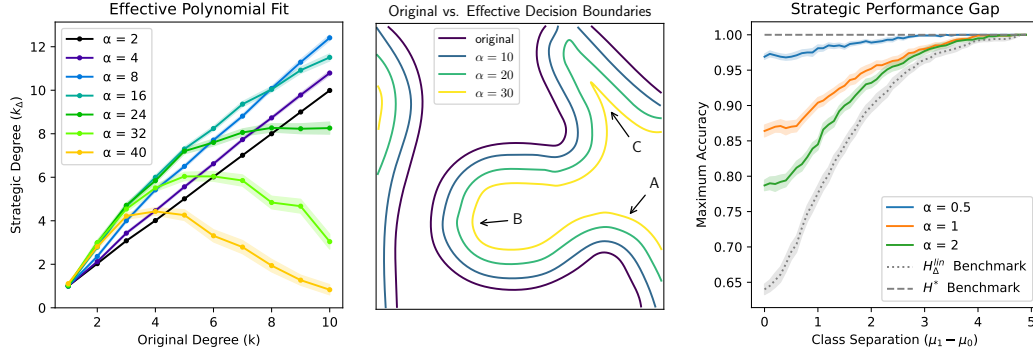


Figure 6: **(Left) Expressivity.** For random polynomial classifiers of degree k , results show the smallest degree k' that captures the effective decision boundary. **(Center)** An instance showing positive curvature decreasing (A), negative curvature increasing (B), and wipeout (C). **(Right) Approximation.** As data becomes more entangled (low separation), strategic approximation degrades.

8 Discussion

This work sets out to explore the interplay between non-linear classifiers and strategic user behavior. Our analysis demonstrates that non-linearity induces behavior that is both qualitatively different than the linear case and also non-apparent by simply studying it. Simply put, the strategic setting is fundamentally limited, though has a few potential advantages. Our results show how such behavior can impact classifiers by morphing the decision boundary and model classes by increasing or decreasing complexity. Although prior work has made clear the importance of accounting for strategic behavior in the learning objective, our work suggests that there is a need for additional broader considerations throughout the entire learning pipeline from the choices we make initially (such as which model class to use) to setting our final expectations (such as the accuracy levels we may aspire to achieve). This motivates future theoretical questions, as well as complementary work on practical aspects such as optimization (i.e., how to solve the learning problem), modeling (i.e., how to capture true human responses), and evaluation (i.e., on real humans and in the wild).

References

- [1] Saba Ahmadi, Hedyeh Beyhaghi, Avrim Blum, and Keziah Naggita. The strategic perceptron. In *Proceedings of the 22nd ACM Conference on Economics and Computation*, pages 6–25, 2021.
- [2] Yahav Bechavod, Chara Podimata, Steven Wu, and Juba Ziani. Information discrepancy in strategic learning. In *International Conference on Machine Learning*, pages 1691–1715. PMLR, 2022.
- [3] Michael Brückner, Christian Kanzow, and Tobias Scheffer. Static prediction games for adversarial learning problems. *The Journal of Machine Learning Research*, 13(1):2617–2654, 2012.
- [4] Michael Brückner and Tobias Scheffer. Nash equilibria of static prediction games. In *Advances in neural information processing systems*, pages 171–179, 2009.
- [5] Yiling Chen, Yang Liu, and Chara Podimata. Learning strategy-aware linear classifiers. *Advances in Neural Information Processing Systems*, 33:15265–15276, 2020.
- [6] Lee Cohen, Yishay Mansour, Shay Moran, and Han Shao. Learnability gaps of strategic classification. 247:1223–1259, 2024. Publisher Copyright: © 2024 L. Cohen, Y. Mansour, S. Moran and H. Shao.; 37th Annual Conference on Learning Theory, COLT 2024 ; Conference date: 30-06-2024 Through 03-07-2024.
- [7] Daniel Cullina, Arjun Nitin Bhagoji, and Prateek Mittal. Pac-learning in the presence of evasion adversaries. In *Proceedings of the 32nd International Conference on Neural Information*

- Processing Systems*, NIPS'18, page 228–239, Red Hook, NY, USA, 2018. Curran Associates Inc.
- [8] Jinshuo Dong, Aaron Roth, Zachary Schutzman, Bo Waggoner, and Zhiwei Steven Wu. Strategic classification from revealed preferences. In *Proceedings of the 2018 ACM Conference on Economics and Computation*, pages 55–70, 2018.
 - [9] Itay Eilat, Ben Finkelshtein, Chaim Baskin, and Nir Rosenfeld. Strategic classification with graph neural networks. In *The Eleventh International Conference on Learning Representations, ICLR 2023, Kigali, Rwanda, May 1-5, 2023*. OpenReview.net, 2023.
 - [10] Itay Eilat and Nir Rosenfeld. Performative recommendation: diversifying content via strategic incentives. In *International Conference on Machine Learning*, pages 9082–9103. PMLR, 2023.
 - [11] Andrew Estornell, Sanmay Das, Yang Liu, and Yevgeniy Vorobeychik. Group-fair classification with strategic agents. In *Proceedings of the 2023 ACM Conference on Fairness, Accountability, and Transparency, FAccT '23*, page 389–399, New York, NY, USA, 2023. Association for Computing Machinery.
 - [12] R. T. Farouki and C. A. Neff. Analytic properties of plane offset curves. *Comput. Aided Geom. Des.*, 7(1–4):83–99, June 1990.
 - [13] Jerome H Friedman. Greedy function approximation: a gradient boosting machine. *Annals of statistics*, pages 1189–1232, 2001.
 - [14] Ganesh Ghalme, Vineet Nair, Itay Eilat, Inbal Talgam-Cohen, and Nir Rosenfeld. Strategic classification in the dark. In *International Conference on Machine Learning*, pages 3672–3681. PMLR, 2021.
 - [15] Alirio Gómez Gómez and Pedro L. Kaufmann. On the Vapnik-Chervonenkis dimension of products of intervals in \mathbb{R}^d . *arXiv e-prints*, page arXiv:2104.07136, April 2021.
 - [16] Moritz Hardt, Nimrod Megiddo, Christos Papadimitriou, and Mary Wootters. Strategic classification. In *Proceedings of the 2016 ACM conference on innovations in theoretical computer science*, pages 111–122, 2016.
 - [17] Kurt Hornik, Maxwell Stinchcombe, and Halbert White. Multilayer feedforward networks are universal approximators. *Neural networks*, 2(5):359–366, 1989.
 - [18] Safwan Hossain, Evi Micha, Yiling Chen, and Ariel Procaccia. Strategic classification with externalities. In *The Thirteenth International Conference on Learning Representations, ICLR 2025, Singapore, April 24-28, 2023, 2025*.
 - [19] Meena Jagadeesan, Celestine Mendler-Dünner, and Moritz Hardt. Alternative microfoundations for strategic classification. In *International Conference on Machine Learning*, pages 4687–4697. PMLR, 2021.
 - [20] Soo Won Kim, Ryeong Lee, and Young Joon Ahn. A new method approximating offset curve by bézier curve using parallel derivative curves. *Computational and Applied Mathematics*, 37(2):2053 – 2064, 2018. Cited by: 3.
 - [21] Anilesh K Krishnaswamy, Haoming Li, David Rein, Hanrui Zhang, and Vincent Conitzer. Classification with strategically withheld data. In *Proceedings of the AAAI Conference on Artificial Intelligence*, volume 35, pages 5514–5522, 2021.
 - [22] Andrey Kupavskii. The vc-dimension of k-vertex d-polytopes. *Combinatorica*, 40(6):869–874, December 2020.
 - [23] Tosca Lechner and Ruth Urner. Learning losses for strategic classification. In *Thirty-Sixth AAAI Conference on Artificial Intelligence, AAAI*, pages 7337–7344. AAAI Press, 2022.
 - [24] Sagi Levanon and Nir Rosenfeld. Strategic classification made practical. In *International Conference on Machine Learning*, pages 6243–6253. PMLR, 2021.

- [25] Sagi Levanon and Nir Rosenfeld. Generalized strategic classification and the case of aligned incentives. In *Proceedings of the 39th International Conference on Machine Learning (ICML)*, 2022.
- [26] J. Park and I. W. Sandberg. Universal approximation using radial-basis-function networks. *Neural Computation*, 3(2):246–257, 1991.
- [27] Elan Rosenfeld and Nir Rosenfeld. One-shot strategic classification under unknown costs. In *Forty-first International Conference on Machine Learning*, 2024.
- [28] Han Shao, Avrim Blum, and Omar Montasser. Strategic classification under unknown personalized manipulation. In *Advances in Neural Information Processing Systems*, volume 36, 2023.
- [29] Yonadav Shavit, Benjamin Edelman, and Brian Axelrod. Causal strategic linear regression. In *International Conference on Machine Learning*, pages 8676–8686. PMLR, 2020.
- [30] Marshall H Stone. The generalized weierstrass approximation theorem. *Mathematics Magazine*, 21(5):237–254, 1948.
- [31] Ravi Sundaram, Anil Vullikanti, Haifeng Xu, and Fan Yao. PAC-learning for strategic classification. In *International Conference on Machine Learning*, pages 9978–9988. PMLR, 2021.
- [32] Aad Vaart and Jon Wellner. A note on bounds for vc dimensions. *Institute of Mathematical Statistics collections*, 5:103–107, 01 2009.
- [33] Tian Xie and Xueru Zhang. Non-linear welfare-aware strategic learning. *Proceedings of the AAAI/ACM Conference on AI, Ethics, and Society*, 7:1660–1671, 10 2024.
- [34] Hanrui Zhang and Vincent Conitzer. Incentive-aware PAC learning. In *Proceedings of the AAAI Conference on Artificial Intelligence*, volume 35, pages 5797–5804, 2021.
- [35] Tijana Zrnic, Eric Mazumdar, Shankar Sastry, and Michael Jordan. Who leads and who follows in strategic classification? *Advances in Neural Information Processing Systems*, 34:15257–15269, 2021.

A Definitions

A.1 Signed Curvature

Our analysis makes use of the notion of *signed curvature* – a signed version of the normal curvature – to quantify shape alteration. Because there is an inherent notion of direction due to the binary nature of label classes, we can define curvature as being positive if the curvature normal vector points in the direction of the positive region and negative if it points in the direction of the negative region. Though in \mathbb{R}^2 this defines a single value, we must instead define a curvature value for each "direction" in higher dimensions. More formally, for each tangent vector \vec{t} in the tangent hyperplane T_x at x , we define the curvature value $\kappa_{\vec{t}}$ as the signed curvature at x on the curve obtained by intersecting the decision boundary with the plane L containing \vec{t} and the normal vector \hat{n}_x . Defining $K = \{\kappa_{\vec{t}} : \vec{t} \in T\}$ as the set of all such curvatures, our analysis will focus on $\kappa^* = \sup(K)$ in \mathbb{R}^3 and above.

B Proofs

Lemma 1. *In \mathbb{R}^2 , if the curvature κ at x is positive, then the radius r_{insc} of the maximum inscribed circle at x is no bigger than the radius $r_{osc} = \frac{1}{\kappa}$ of the osculating circle at x (the circle that best approximates the curve at x and has the same curvature). As a corollary, if curvature κ at x is negative, then the radius r_{esc} of the maximum escribed circle at x is no bigger than the radius $r_{osc} = \frac{1}{-\kappa}$ of the osculating circle at x .*

Proof. Note that both the osculating circle and the inscribed circle have their centers along the normal line to the curve at x (and on the same side of h), and that the osculating circle may cross the curve at x . If it does, then any circle which has a larger radius and a center on the same side of h along the normal line to the curve will also cross the decision boundary at x , so the radius of the inscribed circle is strictly smaller than the radius of the osculating circle. If the osculating circle does not cross the curve, then it must be the largest strictly tangent circle at x or else it would not be the best circular approximation to the curve at x . As such, the largest inscribed circle, which must be both tangent to the curve at x also not intersect it anywhere else, must have a radius that is no larger than r_{osc} . □

B.1 One-to-One Mapping

Claim: *In one-to-one mapping, the point x on the decision boundary of h is mapped to the point $\hat{x} = x - \alpha\hat{n}_x$ on the decision boundary of h_Δ .*

Proof. Note that all points on the decision boundary of h_Δ must be at the maximum cost away from h^4 , so $\nabla_h(x) \subset S_\alpha(x)$. Additionally, for each $x' \in \nabla_h(x)$, the ball $B_\alpha(x')$, which is the set of points that x' can move to, must not intersect the decision boundary of h (or else it would not be at maximum cost away) and must furthermore be strictly tangent to the decision boundary at x . Given that the decision boundary of h is smooth at x , this means that the normal to the curve at x must run along the radius of $B_\alpha(x')$ from x to x' , implying that $x' = x \pm \alpha\hat{n}_x$. Because of the inherit directionality of the setting, the normal vector at x is defined to point in the positive direction. This means that only the point $\hat{x} = x - \alpha\hat{n}_x$ would seek to move to x to gain a positive classification as $x' = x + \alpha\hat{n}_x$ is either already labeled positive or can move to a closer point. Therefore, $\nabla_h(x) = \{x - \alpha\hat{n}_x\}$ in the one-to-one case. □

B.2 Wipeout Mapping

Claim: *Points on the decision boundary of h that are "wiped out" do not affect the effective decision boundary of h_Δ .*

⁴Otherwise, x would not be on the on the boundary of positive and negative classification by h_Δ because all of the points adjacent to it can also strategically move to get a positive classification.

Proof. In the case of *indirect wipeout*, this follows directly from the definition: if $\nabla_h(x)$ is contained in $B_\alpha(x')$ (or in the union of several $B_\alpha(x')$), then none of the points in $\nabla_h(x)$ are at a maximum cost away from h and therefore are not on the decision boundary of h_Δ .

In the case of *direct wipeout*, the normal one-to-one mapping fails because the point $\hat{x} = x - \alpha \hat{n}_x$ is no longer at the maximum cost away from h . Specifically, because the curvature $\kappa < -1/\alpha$ ⁵, the ball $B_\alpha(x')$ now intersects h , which means that x' is less than α away from h . For \mathbb{R}^2 , Lemma 1 proves that the radius of the maximum escribed circle at x is less than the radius of the osculating circle, so $r_{esc} \leq r_{osc} = \frac{1}{-\kappa} < \alpha$. Therefore, $B_\alpha(x')$ must intersect h .

For higher dimensions (see Appendix A.1), there is no longer a single normal curvature. Instead, we define the set K of curvatures in each plane $p \in P$ defined by the normal vector and some tangent vector at x . Note that $B_\alpha(x')$ will intersect h if any of its projections onto each $p \in P$ (a circle) intersects the curve obtained by intersecting the decision boundary with the plane p . Since each of these cases are in \mathbb{R}^2 , $B_\alpha(x')$ will intersect h if $\inf(K) < -1/\alpha$. □

B.3 Proof of Proposition 1

Proposition 1: *Let x be a point on the decision boundary of h with signed curvature $\kappa \geq -1/\alpha$. The effective curvature of the corresponding \hat{x} on the boundary of h_Δ is given by:*

$$\kappa_\Delta = \kappa / (1 + \alpha\kappa) \quad (3)$$

Proof. While an equivalent form of Prop. 1 has already been proven in the field offset curves [12], we nonetheless reprove it here to offer some intuition behind it. In the normal one-to-one mapping, because both the center of curvature and $\nabla_h(x)$ lie on the normal line to h at x , strategic movement can be seen as increasing the signed radius of curvature r_{osc} by α (where we will define the radius of curvature as negative if the curvature is negative at x). In higher dimensions, this is equivalent to increasing each of the radii of curvature by α (see Appendix A.1). We therefore have:

$$\begin{aligned} r_{osc,\Delta} &= r_{osc} + \alpha \\ \kappa_\Delta &= \frac{1}{r_{osc,\Delta}} = \frac{1}{r_{osc} + \alpha} \\ &= \frac{1}{\frac{1}{\kappa} + \alpha} \\ &= \frac{\kappa}{1 + \alpha\kappa} \end{aligned}$$

Note that Eq. 3 has a horizontal asymptote at $\kappa_\Delta = 1/\alpha$ because the effective curvature cannot exceed $1/\alpha$ (see Sec. 5.3). Additionally, Eq. 3 has a vertical asymptote at $\kappa = -1/\alpha$ because any point with lower curvature has no effect on h_Δ (see Appendix B.2). When $\kappa = -1/\alpha$, x is mapped to a non-smooth kink of infinite curvature. □

B.4 Proof of Proposition 2

Proposition 2: *Let g be a candidate classifier. If there exists a point x on the decision boundary of g such that all points $x' \in S_\alpha(x)$ are reachable from some point in $\mathcal{X}_0(g)$, then there is no h such that $g = h_\Delta$.*

Proof. In order for g to be the effective classifier of regular classifier h , we must have:

1. For each point z that is positively classified by g , there must be a point $z' \in B_\alpha(z)$ which is classified as positive by h . In other words, z must be able to acquire a positive label by staying in place or strategically moving within $B_\alpha(z)$.

⁵or $\inf(K) < -1/\alpha$ for $d > 2$. See Sec. 5.1 and Appendix A.1 for curvature definitions

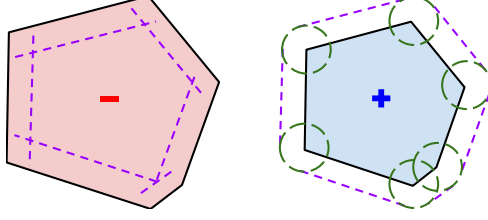


Figure 7: **(Left)** Each face of a negative-inside polytope is mapped to a new linear face, though the resulting h_Δ may be a polytope with fewer faces and vertices due to wipeout. **(Right)** Each face of a positive-inside polytope is also mapped to a new linear face, though each vertex will have to expand to fill the gap between these faces.

2. For each point z that is negatively classified by g , there cannot be any points $z' \in B_\alpha(z)$ which are classified as positive by h . In other words, z must not be able to acquire a positive label by staying in place or strategically moving within $B_\alpha(z)$.

Assume there exists a point x on the decision boundary of g such that all points $x' \in S_\alpha(x)$ are reachable from $\mathcal{X}_0(g)$ and that there exists h such that $g = h_\Delta$. Since x is on the decision boundary of g , there exists a point $x + \delta, \delta \rightarrow 0$ which is negatively classified by g . For requirement 1 and 2 to hold, there must be a point $x' \in S = \{z : z \in B_\alpha(x), z \notin B_\alpha(x + \delta)\}$ that is positively classified by h . Since $S \subset S_\alpha(x)$, we can expand the claim to say that there must be a point $x' \in S_\alpha(x)$ that is positively classified by h . However, if all points $x' \in S_\alpha(x)$ are reachable by some point z that is negatively classified by g , then none of the points $x' \in S_\alpha(x)$ can be positively classified by h (by requirement 2). Therefore, if there exists a point x on the decision boundary of g for which every point on the sphere $S_\alpha(x)$ is reachable by some point that is negatively classified by g , then g cannot be a possible effective classifier. \square

B.5 Proof of Proposition 3

Proposition 3: *Let g be a candidate classifier. If there exists a point x on the decision boundary of g where (i) g is smooth, and (ii) the point $\hat{x} = x + \alpha\hat{n}_x$ is reachable by some $x' \in \mathcal{X}_0(g)$, then there is no h such that $g = h_\Delta$.*

Proof. By proposition 2, for each point x on the decision boundary of g , there must be a point x' on $S_\alpha(x)$ which is classified positively by h and also not reachable by any point negatively classified by g . As a result, the ball $B_\alpha(x')$, which is the set of points that can move to x' , must not intersect the decision boundary and must furthermore be strictly tangent to the decision boundary at x . Given that the decision boundary is smooth at x , this means that the normal to the curve at x must run along the radius of $B_\alpha(x')$ from x to x' , implying that $x' = x \pm \alpha\hat{n}_x$. Because the strategic movement is in the direction of a positive classification, the only possible option for x is to move to $x' = x + \alpha\hat{n}_x$. However, if $x' = x + \alpha\hat{n}_x$ is reachable by some point that is negatively classified by h_Δ , then the associated h would not have classified x' as positive, so x would not have been a positively classified point by h_Δ . \square

B.6 Effective Class of Polytope Family

Each polytope is simply a combination of n linear faces. As such, when a polytope has a negative inside, each face will be mapped to a new linear face (with some wipeout of part or all of the face) leading to an h_Δ that is a smaller-radius polytope, albeit with potentially fewer faces and edges (see Fig. 7 (Left)). Although the faces of a positive-inside polytope also map to new linear faces, each vertex will have to expand to fill the gap between these new faces. As such, h_Δ is now a larger polytope whose corners are partial to a ball (see Fig. 7 (Right)). For the ℓ_1 and ℓ_∞ costs, h_Δ therefore remains a polytope since the ℓ_1 and ℓ_∞ balls are piecewise-linear themselves. For the ℓ_2 cost, h_Δ is now a polytope with rounded corners. In either case, the decision boundary of each $p_\Delta^k \in P_\Delta^k$ can be seen as the intersection of a radius-scaled p^k and k balls centered at each vertex of p^k .

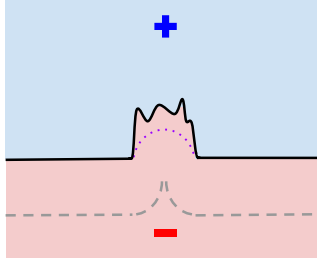


Figure 8: Example h from a class H where $\text{VC}(H) = \infty$, but $\text{VC}(H_\Delta) = 0$. The grey dashed curve is the h_Δ of any h like the one above with the same small gap where the decision boundary remains above the dotted purple line.

B.7 Proof of Proposition 4

Proposition 4: For each class Q_s^k of negative-inside k -vertex polytopes bounded by a radius of s , $\text{VC}(Q_s^k) \geq \text{VC}(Q_{s,\Delta}^k)$. Moreover, if $s = \infty$, then $\text{VC}(Q_s^k) = \text{VC}(Q_{s,\Delta}^k)$ as implied by Thm. 2.

Proof. As noted in Appendix B.6, negative-inside polytopes map to smaller-radius negative-inside polytopes with potentially fewer faces and vertices. As such $Q_{s,\Delta}^k \subset Q_s^k$, so $\text{VC}(Q_{s,\Delta}^k) \leq \text{VC}(Q_s^k)$. However, if $s = \infty$, the class Q_s^k is closed to input scaling leading to $\text{VC}(Q_{s,\Delta}^k) \geq \text{VC}(Q_s^k)$ by Thm. 2, so we must have that $\text{VC}(Q_{s,\Delta}^k) = \text{VC}(Q_s^k)$. \square

B.8 Proof of Theorem 1

Theorem 1: There exist several model classes H where $\text{VC}(H) = \infty$, but $\text{VC}(H_\Delta) = 0$.

Proof. We provide two examples. For the first example, fix $\alpha < 1$ and consider the class of \mathbb{R}^2 classifiers $H = \{h_S \mid S \subseteq \mathbb{Z}^2\}$ where $h_S = \mathbb{1}\{x \notin B_{\alpha-\delta}(z) \forall z \in S\}$. Each classifier in this model class contains small, non-overlapping negative regions centered at lattice points. Thus, the negative regions of all $h \in H$ will disappear under strategic movement leaving $h_\Delta(x) = 1 \forall h \in H$. Despite the fact that H shatters \mathbb{Z}^2 (and therefore has $\text{VC}(H) = \infty$), H_Δ cannot shatter a single point (and therefore has $\text{VC}(H_\Delta) = 0$).

Another example where h_Δ is perhaps more natural can be seen in Fig. 8. In this case, H is the class of classifiers whose decision boundaries can be written as

$$h_i((x_1, x_2)) = \begin{cases} 0 & x_1 \leq -k, \\ f_i((x_1, x_2)) & -k \leq x_1 \leq k \\ 0 & x_1 \geq k \end{cases} \quad (4)$$

where k is some constant less than α and each function $f_i((x_1, x_2))$ satisfies $f_i((x_1, x_2)) \geq \alpha^2 - x_1^2 - x_2^2$ for all $-k \leq x_1 \leq k$. In this case, decision boundary points in the gap will get wiped out on all $h \in H$ leaving the exact same h_Δ . Because H is nearly unrestricted in the range $-k \leq x_1 \leq k$, it is capable of shattering infinite points that lie in this range and has infinite VC dimension. On the other hand, because $|H_\Delta| = 1$, we get $\text{VC}(H_\Delta) = 0$. \square

B.9 Proof of Theorem 2

Definition 1. A hypothesis class H is said to be closed to input scaling if for all $h(x) \in H$ and for all $a > 0$, we have that $h_a(x) = h(ax) \in H$ as well.

Note that the family of polynomials and polytopes are clearly closed to input scaling. Furthermore, most classes of neural networks are as well since $h(ax)$ can be realized by scaling the first weight vector by a .

Theorem 2: If H is closed under input scaling and $\text{VC}(H) < \infty$, then $\text{VC}(H) \leq \text{VC}(H_\Delta)$.

Proof. Intuitively, the reason that the VC dimension cannot decrease is that for any H with VC dimension k that is closed to input scaling, we can find a set S of k point that can be shattered by H where none of the points $s \in S$ strategically move under any of the $h \in H$ used to shatter S . As a result, H_Δ will also shatter S so its VC dimension is at least k .

Let $\text{VC}(H) = k$ and $G \subset H$ be a set of 2^k classifiers that shatters some set S of k points. Define $c_{DB}(s, g)$ as the minimum strategic cost necessary for point s to obtain a positive classification from classifier g and define $c_{neg}(S, G)$ as the minimum strategic cost for any $s \in S$ to obtain a positive classification from a classifier $g \in G$ that classifies s negatively:

$$c_{neg}(S, G) = \min_{s \in S, g \in G, g(s)=0} c_{DB}(s, g) \quad (5)$$

Since both S and G are finite sets and negative points face a strictly positive cost to obtain a positive classification, we get that $c_{neg}(S, G) > 0$. Additionally, because the VC dimension is indifferent to input scaling⁶, if we scale both the classifiers and the points, then $G' = \{g(ax) : g(x) \in G\}$ will shatter $S' = \{ax : x \in S\}$ with $c_{neg}(S', G') = a \cdot c_{neg}(S, G)$. Note that because H is closed to input scaling, $G' \subset H$ as well. Furthermore, if we choose $a = \frac{\alpha+1}{c_{neg}(S, G)}$, then $c_{neg}(S', G') = \alpha + 1$. Note that if $c_{neg}(S', G') > \alpha$, no point $s' \in S'$ will move strategically under any $g' \in G'$, meaning that $g'_\Delta(s') = g'(s') \forall g' \in G', s' \in S'$. As a result, G'_Δ will also shatter S' so $\text{VC}(G'_\Delta) \geq |S'| = k$. Since $G'_\Delta \subset H_\Delta$, we get that

$$\text{VC}(H_\Delta) \geq \text{VC}(G'_\Delta) \geq k = \text{VC}(H) \quad (6)$$

□

B.10 Proof of Theorem 3

Theorem 3: Consider either the ℓ_1 , ℓ_2 , or ℓ_∞ costs and let $H \subseteq P^k$, where P^k is the set of all k -vertex polytopes in R^d . Then $\text{VC}(H_\Delta) = O(kd^2 \log k)$.

Proof. We will make use of the following known results:

Lemma 2 (Gómez and Kaufmann (2021)). Let H^{Ball} be the class of all ℓ_p balls in R^d . Then H^{Ball} has VC dimension $\text{VC}(H^{Ball}) = \Theta(d)$ for $p = 1, 2$, or ∞ [15].

Lemma 3 (Vaart and Wellner (2009)). Let classes C_1, C_2, \dots, C_k have VC dimensions V_1, V_2, \dots, V_k and $V = \sum_{i=1}^k V_i$. Let $C_U = \bigcup_i C_i$ and Let $C_I = \bigcap_i C_i$. Then both C_U and C_I have VC dimension upper bounded by $O(V \cdot \log(k))$ [32].

We note that by combining Lemmas 2 and 3, the class H_k^{Ball} of the union of k ℓ_1, ℓ_2 , or ℓ_∞ balls has a VC dimension of $O(k d \log(k))$. As seen in Appendix B.6, the effective classifier of a k -vertex positive-inside polytope is the intersection of a larger radius k -vertex positive-inside polytope and k ℓ_p balls centered at each of the vertices. Therefore, $H_\Delta \subset P^k \cap H_k^{ball}$ so :

$$\begin{aligned} \text{VC}(H_\Delta) &\leq \text{VC}(P^k \cap H_k^{ball}) \\ &= O(\text{VC}(P^k) + \text{VC}(H_k^{ball})) \\ &= O(k d^2 \log(k)) + O(k d \log(k)) \\ &= O(k d^2 \log(k)) \end{aligned}$$

□

⁶Input scaling only changes the distance between points, but does not change their relative positions, so the class H and its input scaled class H' will have the same VC dimension.

B.11 Proof of Proposition 5

Proposition 5: For all d , there exist (non-degenerate) distributions on \mathbb{R}^d that are realizable in the standard setting, but whose strategic accuracy is the majority class rate, $\max_y p(y)$.

Proof. Fix d and choose any arbitrary set of positive points \mathcal{X}_1 . When $d = 1$, the set of negative points \mathcal{X}_0 can be constructed by placing a negative point δ to the left and right of each positive point. When $d > 1$, this generalizes to selecting $d + 1$ points around each positive point $x \in \mathcal{X}_1$ that form an \mathbb{R}^d tetrahedron $T_\delta^d(x)$ ⁷. In this case, the classifier $h(x) = \mathbf{1}\{x \in \mathcal{X}_1\}$ achieves perfect standard accuracy, and the classifier that classifies all points as negative will achieve a strategic accuracy of $\frac{d+1}{d+2}$. Note that for each point z in space to which $x \in \mathcal{X}_1$ can strategically move, there exists at least one $x' \in T_\delta^d(x)$ that can as well. Therefore, for each positive point $x \in \mathcal{X}_1$ that achieves a correct positive classification by strategically moving to z (z can be the same as x if it doesn't move), there is a unique negative point $x' \in T_\delta^d(x)$ that achieves an incorrect negative classification by strategically moving to z , so the strategic accuracy does not benefit from correctly classifying any positive points. \square

B.12 Proof of Proposition 6

Proposition 6: There exists a distribution which is realizable in the standard setting, but whose accuracy under any h_Δ is at most $0.5 + \frac{1}{\lfloor 2\alpha + 1 \rfloor}$.

Proof. Consider set of lattice points in \mathbb{R}^1 with alternating labels. Although $f(x) = \sin(\pi x)$ achieves perfect standard accuracy on this distribution, we will show that the maximum strategic accuracy for any model class is $0.5 + \frac{1}{\lfloor 2\alpha + 1 \rfloor}$, which approaches 0.5 as $\alpha \rightarrow \infty$. Note that in \mathbb{R}^1 , the minimum size of a positive interval is 2α . Additionally, for each positive interval I of length k , I will contain either $\lfloor k \rfloor$ or $\lfloor k \rfloor + 1$ points and include at most one more positive point than negative point. Therefore, each interval I will at best be correct on $\frac{\lfloor k \rfloor + 1}{2}$ out of $\lfloor k \rfloor$ points, which is optimized for $k = 2\alpha$ (i.e. the minimum possible value of k). Furthermore, because the negative intervals may also only have at most one more negative point than positive point, the negative intervals are optimized when they include only a single negative point. As such, an optimal strategic classifier h consists of repeated positive intervals that includes $\lfloor 2\alpha \rfloor$ points followed by a negative interval that includes one negative point. For each positive and negative interval group, h correctly classifies at most $\frac{\lfloor 2\alpha \rfloor + 1}{2} + 1$ out of $\lfloor 2\alpha + 1 \rfloor$ points correctly for an overall maximum accuracy of $\frac{\frac{\lfloor 2\alpha \rfloor + 1}{2} + 1}{\lfloor 2\alpha + 1 \rfloor} = 0.5 + \frac{1}{\lfloor 2\alpha + 1 \rfloor}$. \square

C Additional results

C.1 Partial Expansion

As seen in Fig. 9 (Left), partial expansion may occur if part of the expansion artifact is discarded through *indirect wipeout*. In the figure, part of the artifact (gold) is within α of the upper positive region and therefore does not become part of the decision boundary.

C.2 Merging/Splitting Regions

As seen in Fig. 9 (Right), two positive regions can merge together when they are separated by a narrow pass in h . If the narrow pass is part of a larger negative region, the region will be split in two, which can potentially increase the complexity of the decision boundary (for example in Fig. 9 (Left)).

C.3 Types of Impossible Effective Classifiers

As stated in Sec. 5.3, we identify four "types" of classifiers g that cannot exist as effective classifiers. Formally, these classifiers are ones which include either:

⁷We can assume without loss of generality that $\bigcap_{x_1, x_2 \in \mathcal{X}_1} T_\delta^d(x) = \emptyset \forall x_1, x_2 \in \mathcal{X}_1$ since there are infinite options for each T_δ^d and we can just pick ones that do not overlap.

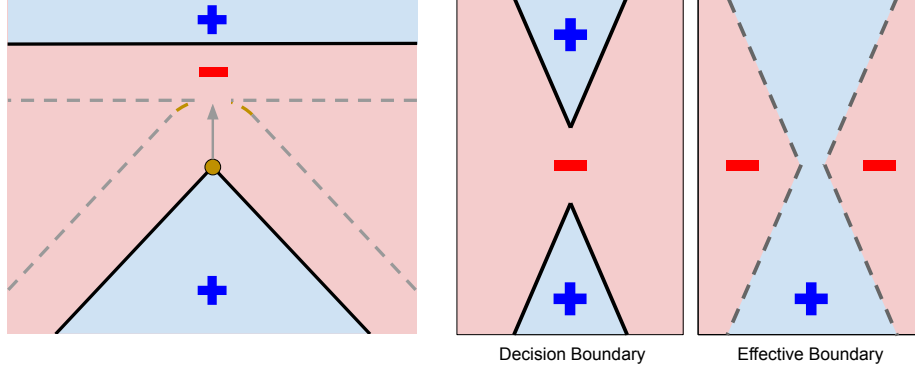


Figure 9: **(Left)**: Partial expansion. **(Right)**: Regions merging/splitting

1. A small continuous region of positively classified points C where $\exists z \in \mathbb{R}^d$ such that $x \in B_\alpha(z) \forall x \in C$.
2. A narrow continuous region C where all points are classified as positive and are α -close to the decision boundary.
3. A smooth point on the decision boundary which has signed curvature $\kappa > 1/\alpha$ (or $\kappa^* > 1/\alpha$ when $d > 2$).
4. A locally convex intersection of piecewise linear or hyperlinear segments.

Note that the first case is just a special case of the second case. Nonetheless, we have separated them to emphasize that the impossible positive regions can either be fully or partially contained.

Cases 1 and 2: Small/Narrow Positive Regions

Let $x \in C$ be some point in a small positive region in g . For x to be classified as positive, there must be a point $x' \in B_\alpha(x)$ which is classified positively by h and not reachable by any $z \in \mathcal{X}_0(h)$ (see requirements 1 and 2 in Appendix B.4). However, any point $x' \in B_\alpha(x) \cap C$ is reachable by $\mathcal{X}_0(h)$ and any point $x' \in B_\alpha(x) \cap C^c$ is also reachable by $\mathcal{X}_0(h)$ since it is closer to some $z \in \mathcal{X}_0(h)$ than to x . Therefore, there are no points $x' \in B_\alpha(x)$ which are not reachable by any $z \in \mathcal{X}_0(h)$, so g cannot be an effective classifier.

Case 3: Large positive curvature

We will show that any g with directional curvature greater than $1/\alpha$ anywhere on the decision boundary will fail Prop. 3. In other words, if the directional curvature at point x is greater than $1/\alpha$, then the point $x + \alpha \hat{n}_x$ will be reachable by some point that is negatively classified by g . In order for the point $x + \alpha \hat{n}_x$ to be reachable by x but not any point negatively classified by g , the ball $B_\alpha(x + \alpha \hat{n}_x)$ – which is the set of points that can strategically move to $x + \alpha \hat{n}_x$ – must not intersect g and must also be strictly tangent to it at x . However, if the curvature at point x is greater than $1/\alpha$, then the maximum radius r_{insc} of a ball that is strictly tangent to x is less than α so g does not meet Prop. 3.

In \mathbb{R}^2 , Lemma 1 proves that the radius r_{insc} of the maximum inscribed circle at x is no bigger than the radius $r_{osc} = \frac{1}{\kappa}$ of the osculating circle at x . We therefore have that $r_{insc} \leq r_{osc} = \frac{1}{\kappa} < \alpha$. In higher dimensions (see Appendix A.1), there is no longer a single normal curvature. Instead, we define the set K of curvatures in each plane $p \in P$ defined by the normal vector and some tangent vector at x . Note that $B_\alpha(x + \alpha \hat{n}_x)$ is only strictly tangent to the decision boundary at x if its intersection with each $p \in P$ (a circle) is strictly tangent at x to the curve obtained by intersecting the decision boundary with the plane p . Since each of these cases are in \mathbb{R}^2 , each one will only hold if the curvature at x in p is no more than $1/\alpha$. Therefore, if $\kappa^* = \sup(K) > 1/\alpha$ for any x on the decision boundary, then the maximum radius of a ball that is strictly tangent to x is less than α , so g does not meet Prop. 3.

Case 4: Piecewise Linear Segments

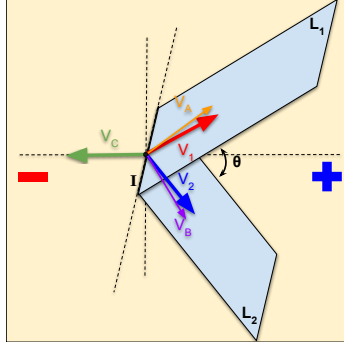


Figure 10: Diagram for proof of case 4.

Lemma 4. *The set of points which are reachable by point x but not point $x + \delta\vec{v}$ for unit vector \vec{v} and $\delta \rightarrow 0$ all satisfy $\vec{v} \cdot x \leq 0$.*

Proof (Lemma 4). Define an orthonormal basis v_1, v_2, \dots, v_d with $v_1 = v$. For any point y such that $\vec{v} \cdot y > 0$, the vector connecting x and y can be written as $a_1v_1 + a_2v_2 + \dots + a_dv_d$ while the vector connecting $x + \delta\vec{v}$ and y can be written as $(a_1 - \delta)v_1 + a_2v_2 + \dots + a_dv_d$. Since $\delta < a_1$, y is closer to $x + \delta\vec{v}$ than x . Therefore, any point that is reachable by x and not by $x + \delta\vec{v}$ must satisfy $\vec{v} \cdot x \leq 0$. \square

Proof (Case 4). As depicted in Fig. 10, let L_1 and L_2 be two R^d hyperplane segments that intersect on the decision boundary of g at the R^{d-1} hyperplane segment I , and let x be some point on I . Let $0 < \theta < \pi$ be the angle between L_1 and L_2 on the positive side. Let \vec{v}_1 be the unit vector in L_1 that runs through x and is orthogonal to I ; \vec{v}_2 be the unit vector in L_2 that runs through x and is orthogonal to I ; and $\vec{v}_C = -\frac{\vec{v}_1 + \vec{v}_2}{\|\vec{v}_1 + \vec{v}_2\|}$. Note that for $\delta \rightarrow 0$ the points $x_1 = x + \delta\vec{v}_1$ and $x_2 = x + \delta\vec{v}_2$ are on the decision boundary while the point $x_{12} = x + \delta\vec{v}_C$ is classified as positive and $x_C = x - \delta\vec{v}_C$ is classified as negative. Additionally, if we define \vec{v}_A as the result of \vec{v}_1 being rotated $\epsilon < \frac{\pi - \theta}{2}$ around I away from the positive region and \vec{v}_B as the result of \vec{v}_2 being rotated ϵ around I away from the positive region, then both $x_A = x + \delta\vec{v}_A$ and $x_B = x + \delta\vec{v}_B$ are classified as negative.

Assume that there exists a classifier h associated with the effective classifier g . Therefore, there exists a point y that is reachable to x but not to x_A , x_B , or x_C (which are classified as negative by g). By Lemma 4, any point y that is reachable under strategic movement by point x but not x_A , x_B , or x_C must at least satisfy $y \cdot \vec{v}_A \leq 0$, $y \cdot \vec{v}_B \leq 0$, and $y \cdot \vec{v}_C \leq 0$. However, because $\vec{v}_A + \vec{v}_B$ points in the same direction as $\vec{v}_1 + \vec{v}_2$ – and therefore the opposite direction of \vec{v}_C – we must have that $y \cdot \vec{v}_C = 0$ and $y \cdot (\vec{v}_A + \vec{v}_B) = 0$, which implies that both $y \cdot \vec{v}_A = 0$ and $y \cdot \vec{v}_B = 0$. However, this implies that the vector \vec{y} is orthogonal to both \vec{v}_A and \vec{v}_B , which can only happen if y lies on I or if the angle between \vec{v}_A and \vec{v}_B is either 0 or π . In the former case, y is then reachable by the negatively classified point that is just over the decision boundary from it. The latter case is also not an option because the angle between \vec{v}_A and \vec{v}_B is $\theta_{AB} = \theta + 2\epsilon$ and we have ensured that $0 < \theta + 2\epsilon < \theta + 2\frac{\pi - \theta}{2} = \pi$. In either case, it is impossible for g to classify x as positive while classifying x_A , x_B , and x_C as negative, so there is no h such that $g = h_\Delta$. \square

C.4 Non-bijectiveness of Classifier Mapping

In Sec. 5.3, we show that the mapping $h \mapsto h_\Delta$ is not surjective by showing that there are many potential h_Δ with no associated h . Here, we will show that $h \mapsto h_\Delta$ is also not injective since many classifiers map to the same effective classifier. Furthermore, we show that there are actually infinite h that map to nearly all possible h_Δ . Though there are many more interesting examples, the simplest case of non-injectiveness can be seen by considering an h that includes a continuous positive region C , where $|C| = \infty$. Define the classifier h^x as the classifier that is identical to h except that h^x classifies $x \in C$ as negative instead of positive. Because point x will achieve a positive classification through strategic movement, h_Δ^x is unaffected by x and is the same as h_Δ . Moreover, $h_\Delta^x = h_\Delta$ is true of any $x \in C$, so as long as any h that maps to h_Δ contains a positive region with infinite points, then h_Δ will have infinite h that all map to it. Because positive points in h map to positive

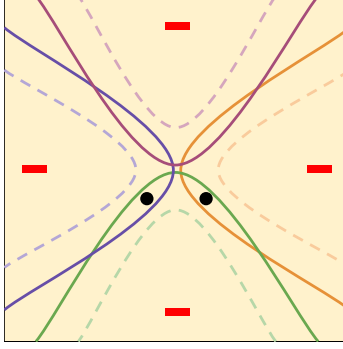


Figure 11: Example of VC decreasing from 2 to 1. Though the black points can be shattered by H , none of the h_Δ overlap so $VC(H_\Delta) = 1$

radius- α balls in h_Δ , any h_Δ with a positive region C such that $\exists x : B_\alpha(x) \subset C$ will have infinite h that all map to it. Note that since all positive regions in h_Δ have a minimum size requirement $\exists x : B_\alpha(x) \subseteq C$, the aforementioned requirement covers all but the h_Δ with absolute minimum-size positive regions.

C.5 Classes with $H = H_\Delta$

Though $H \neq H_\Delta$ for most classes H , there are a few rather simple H other than the class of linear functions where $H = H_\Delta$. For example, under any ℓ_p norm cost, an ℓ_p ball with a positive inside will grow by a radius of α , while an ℓ_p ball with a negative inside will shrink by a radius of α (at least until the radius hits 0). Therefore, many model classes of the subsets of the ℓ_p balls – including the entire class of ℓ_p balls, the class of all negative-inside balls, and the class of balls with a radius that is a multiple of α – all have $H = H_\Delta$ for any fixed α .

Additionally, since each line segment and ℓ_p arc maps to another line segment or ℓ_p arc, many peicewise-linear or peicewise ℓ_p arc classes will also have $H = H_\Delta$. For example, any concave linear intersection will be mapped to a shifted concave linear intersection, so the class of concave linear intersection satisfies $H = H_\Delta$.

C.6 Classes with $VC(H) > VC(H_\Delta) > 0$

There are a couple of mechanisms that can lead to a VC decrease. In the first mechanism, multiple different h have the same h_Δ leading to a smaller and less expressive H_Δ . Two such cases are shown in Appendix B.8 to prove that the VC may decrease even from ∞ to 0. In a similar fashion, we can build an H where only some (instead of all) of the $h \in H$ have the same h_Δ , which would decrease the VC dimension to a non-zero effective VC dimension.

In the second mechanism, the VC can change due to effective classifiers gaining or losing overlap from strategic movement. As the dual to Fig. 5 (Left) where the VC *increases* from 1 to 2 due to this mechanism, Fig. 11 presents an example where the VC *decreases* from 2 to 1. Here, H includes 4 overlapping classifiers with $VC(H) = 2$, yet under strategic behavior, the effective classifiers cease to overlap decreasing the shattering capacity to 1.

C.7 Example of H_Δ with $VC(H_\Delta) = \Theta(d \cdot (VC(H)))$

Claim: *There exists a class H with $VC(H_\Delta) = \Theta(d \cdot (VC(H)))$.*

Proof. For simplification of notation, we build on the case shown in Fig. 5 (Left) using classifiers h that classify some ball as positive and all other points as negative. Note that a similar proof can be built based on a class H of point classifiers [7], but we have decided to include the following construction since classifiers that classify only a single point as positive are quite unrealistic. Let set $S = \mathbb{Z}_2^d - \{0^d\} + \{-\delta^d\}$ be the set of \mathbb{Z}_2^d lattice points with the point $\{0^d\}$ replaced by the point $\{-\delta^d\}$. Consider the case where $\alpha = 0.75$ and $H = \{B_{0.25}(x) : x \in S\}$ is the class of radius-0.25

balls around the points in S . Because the radius of positive balls expand by α under strategic movement, we get that $H_\Delta = \{B_1(x) : x \in S\}$. Note that because none of the balls in H overlap, $\text{VC}(H) = 1$. On the other hand, the balls in H_Δ do overlap allowing H_Δ to shatter the set of d one-hot points $E = \{e_i : i \in [1..d]\}$, where e_i denotes the point with a 1 in the i th coordinate and 0's elsewhere. Note that for each $x \in S - \{-\delta^d\}$, the ball $B_1(x) \in H_\Delta$ classifies E according to the sign pattern x . Additionally, the ball $B_1(-\delta^d)$ does not classify any point in E as positive, so H_Δ covers all 2^d sign patterns of E . As such, $\text{VC}(H_\Delta) \geq d$. However, since $H_\Delta \subset B = \{B_1(x) : x \in R^d\}$, we get that $\text{VC}(H_\Delta) \leq \text{VC}(B) = d + 1$ [15] giving $\text{VC}(H_\Delta) = \Theta(d \cdot (\text{VC}(H)))$. \square

C.8 Example of Strategic Accuracy Exceeding Standard Accuracy

Claim: *In the unrealizable setting, the maximum strategic accuracy can exceed the maximum standard accuracy.*

Proof. In the unrealizable setting, the the maximum strategic accuracy can exceed the maximum standard accuracy when strategic movement helps correct the incorrect classification of positive points. For example, consider a basic setup where $\alpha = 1$, $X = \{(-1, 0), (1, 0), (3, 0)\}$, $Y = \{0, 0, 1\}$, and $H = \{h_1(x) = \text{sign}(x_1 + x_2), h_2(x) = \text{sign}(x_1 - x_2)\}$. In the standard case, both h_1 and h_2 correctly classify the first and third points, but not the second point. However, in the strategic setting, the second point is able to obtain a positive classification under either classifier, so the maximum strategic accuracy is 1. \square

D Experimental details

D.1 Experiment #1: Expressivity

In Sec. 7.1, we experimentally demonstrate how the strategic setting affects classifier expressivity. In this experiment, we first randomly sample a degree- k polynomial h , then determine the set of points S that make up the decision boundary of h_Δ (i.e. are directly adjacent to it), and finally find the best approximate polynomial fit of S . Because user features are often naturally bounded, we assume that $x \in \mathcal{X} = \mathbb{R}^2$ and that all x are bounded by $|x|_\infty \leq 100$. We report average values and standard error confidence intervals of 100 instances of the setup for each $\alpha \in \{2, 4, 8, 16, 24, 32, 40\}$ and $k \in [1, 10]$. The instances were divided among 100 CPUs to speed up computation.

To randomly sample polynomials of degree k , we leverage the fact that the number of points needed to uniquely determine a degree- k polynomial over \mathbb{R}^2 is $\binom{k+2}{2}$. Therefore, for each instance, we randomly choose $\binom{k+2}{2}$ points and labels, and use an SVM polynomial fitter to find the best fitting degree- k polynomial fit to these points. To assure that the generated polynomial is indeed a full-degree polynomial, we construct a grid G of points over $[-100, 100]^2$, label each point $g \in G$ using h to get labels Y , and verify that the SVM best-fitting degree- k polynomial achieves near perfect accuracy on (G, Y) , while the best $(k - 1)$ -degree polynomial achieves low accuracy on (G, Y) .

To find the set of points S that make up the decision boundary of h_Δ , we first strategically label each $g \in G$ by checking if g can reach any point g' that is classified as positive by h . To determine the points that make up the decision boundary of h_Δ , we select only the points $g \in G$ where g and at least one of its direct neighbors are labeled differently by h_Δ .

Finally, we again use an SVM polynomial fit to determine the best approximate polynomial degree of h_Δ . Because the h_Δ of a polynomial is not necessarily a polynomial itself, we set k' to be the lowest degree of the polynomial whose fit on S passes a set tolerance threshold. Empirical tests showed that a tolerance of 0.9 was high enough to ensure a good fit on all of G , but not so high that the SVM fit algorithm needlessly increased the degree just to get a complete overfit to S .

D.2 Experiment #2: Approximation

In Sec. 7.2, we experimentally demonstrate the effects non-universality on the maximum strategic accuracy. This experiment consists of (i) sampling synthetic data and (ii) calculating the maximum linear accuracy and strategic accuracy on each dataset instance. We report average values and standard

error confidence intervals of 20 instances of the setup for each $\alpha \in \{0.5, 1, 2\}$ and $\mu \in [0, 5]$. The instances were divided among 100 CPUs to speed up computation.

For each instance, we generate synthetic \mathbb{R}^2 data by sampling points from class-conditional Gaussians $x \sim N(y\mu, 1)$, where μ is the separation between the centers of each class. Because we were unable to find a polynomial-time algorithm to calculate the maximum accuracy of H_{Δ}^* , exactly 25 points were drawn from each class (denote the full dataset \mathcal{X}). Though this setup may not reflect all possible data distributions, it does represent how the strategic environment behaves under increasing data separability.

To calculate the maximum linear accuracy in each instance, we first note that there exists an optimal linear classifier that runs through (or infinitesimally close to for negative points) exactly two dataset points. This is because for any optimal classifier h that runs through exactly one dataset point $x \in \mathcal{X}$, h may be rotated until it runs through another $x' \in \mathcal{X}$ without changing any of the labels. For any optimal classifier h that runs through no $x \in \mathcal{X}$, h can be shifted until it runs through one (or two collinear) $x \in \mathcal{X}$ and then rotated appropriately. Because all data points are random, we assume that no three points are collinear. Therefore, the maximum linear accuracy on \mathcal{X} can be calculated by taking the maximum accuracy over the $\binom{n}{2}$ classifiers that run through each pair of $x, x' \in \mathcal{X}$ ⁸.

When calculating the maximum strategic accuracy, we note that the minimum size of a positive region in h_{Δ} is the ball B_{α} , so any strategic classifier can be represented by the intersection of multiple B_{α} . We therefore calculate all possible subsets $s \subseteq \mathcal{X}$ that any B_{α} classifies as positive and find the intersection $\bigcap_{s \in S' \subseteq S} s$ with the highest accuracy. To find all $s \in S$, we iterate through the circles centered at each point on a fine-grained grid over the range of the dataset (padded by α on all sides) and check which points $x \in \mathcal{X}$ each circle includes. To find the best intersection of these circles, we iterate through each of the subsets of $Z \subseteq \mathcal{X}_0$ ⁹ and then $s \in S$ to find the maximum number of positive points that can be classified as positive if we allow ourselves to mistakenly classify the negative points in Z .

⁸Because points on the decision boundary are labeled as positive, we manually include that negative points used to define the linear classifier are accurately labeled to reflect the fact that the optimal classifier does not run through the point, but infinitely close to it.

⁹Subsets are traversed in size order with early stopping once the size of the subset is large enough that the accuracy will be worse than the current best accuracy even if all positive points are correctly classified.